Lasers Med Sci (2014) 29:147–156
DOI 10.1007/s10103-013-1302-9

ORIGINAL ARTICLE

# Low-level laser therapy enhances the expression of osteogenic factors during bone repair in rats

**Carla Roberta Tim · Karina Nogueira Zambone Pinto · Bruno Rafael Orsini Rossi · Kelly Fernandes · Mariza Akemi Matsumoto · Nivaldo Antonio Parizotto · Ana Claudia Muniz Rennó**

Received: 8 November 2012 / Accepted: 5 March 2013 / Published online: 21 March 2013


**Abstract** The aim of this study was to evaluate the effects of low-level laser therapy (LLLT) on bone formation, immunoexpression of osteogenic factors, and biomechanical properties in a tibial bone defect model in rats. Sixty male Wistar rats were distributed into bone defect control group (CG) and laser irradiated group (LG). Animals were euthanized on days 15, 30, and 45 post-injury. The histological and morphometric analysis showed that the treated animals presented no inflammatory infiltrate and a better tissue organization at 15 and 30 days postsurgery. Also, a higher amount of newly formed bone was observed at 15 days postsurgery. No statistically significant difference was observed in cyclooxygenase-2 immunoexpression among the groups at 15, 30, and 45 days in the immunohistochemical analysis. Considering RUNX-2, the immunoexpression was statistically higher in the LG compared to the CG at 45 days. BMP-9 immunoexpression was significantly higher in the LG in comparison to CG at day 30. However, there was no expressivity for this immunomarker, both in the CG and LG, at the day 45 postsurgery. No statistically significant difference was observed in the receptor activator of nuclear factor kappa-B ligand immunoexpression among the groups in all periods evaluated. No statistically significant difference among the groups was observed in the maximal load in any period of time. Our findings indicate that laser therapy improved bone healing by accelerating the development of newly formed bone and activating the osteogenic factors on tibial defects, but the biomechanical properties in LG were not improved.

**Keywords** Bone repair · Bone defect · Low-level laser therapy · LLLT

C. R. Tim · N. A. Parizotto
Department of Physiotherapy, Federal University of São Carlos, Rod Washington Luis, Km 235, São Carlos, São Paulo, Brazil

K. N. Z. Pinto
Department of Morphology and Pathology, Federal University of São Carlos, Rod Washington Luis, Km 235, São Carlos, São Paulo, Brazil

B. R. O. Rossi
Departments of Biomechanics and Rehabilitation, University of São Paulo, Av. Bandeirantes, 3.900, Ribeirão Preto, São Paulo, Brazil

K. Fernandes · A. C. M. Rennó (✉)
Department of Bioscience, Federal University of São Paulo, Av. Ana Costa, 95, Vila Mathias, Santos 11050-240 São Paulo, Brazil
e-mail: a.renno@unifesp.br

M. A. Matsumoto
Department of Oral Maxillofacial Surgery, School of Dentistry, University of the Sacred Heart, R. Irmã Arminda, 10-50, Bauru, São Paulo, Brazil

## Introduction

Innovative clinical approaches to repair damage to bone tissue are being developed, including low-level laser therapy (LLLT) [1]. Particularly, LLLT is a common modality used to treat many muscle skeletal conditions and it seems to have an ostegenic potential [2–4]. Biostimulatory effects of LLLT on bone cells have been reported in vivo [1, 4] and in vitro studies [2, 5].

In recent in vitro investigations, Fujimoto et al. [5] and Kiyosaki et al. [6] observed that LLLT stimulated bone nodule formation, accelerated cellular proliferation and differentiation, increased alkaline phosphatase (ALP) activity and upregulated osteocalcin, RUNX-2, and BMP expression in osteoblast cells. Also, LLLT was able to accelerate the

process of fracture repair in rats with a higher maximum load, which indicates its ability to enhance bone resistance [1]. Fávaro-Pipi et al. [4] showed that the 830 nm laser had a positive effect on bone repair, producing a higher amount of newly formed bone and an increase in vascularization at the site of the fracture. Similarly, Ribeiro and Matsumoto [7] found an upregulation of cyclooxygenase-2 (COX-2) expression in bone cells after laser irradiation and an improvement of bone repair in tibial bone defects of rats. Moreover, it seems that LLLT is able to increase the expression of BMP-4, ALP, and RUNX-2 genes during the process of bone healing in rats [3].

Although, in vitro and in vivo data on the irradiation of bone defects by LLLT are encouraging, there is a clear need to understand the cellular and molecular modifications induced by this therapy that control bone formation. In view of the aforementioned, it was hypothesized that the treatment of bone defects with laser therapy could accelerate tissue metabolism and upregulate the synthesis of immunomarkers related to bone healing and bone cell proliferation, providing a treatment with additional advantages for clinical use. Consequently, the present study aimed to evaluate the temporal modifications of LLLT on newly formed bone, immunoexpression of the osteogenic factors (COX-2, RUNX-2, BMP-9, and receptor activator of nuclear factor kappa-B ligand (RANKL)), and in the maximum load of the callus in a tibial bone defect model in rats. To this end, rats were submitted to a tibial bone defect and distributed into control and laser-treated groups. Bone repair was evaluated in different stages (15, 30, and 45 days post-injury), through a histopathological, immunohistochemistry and biomechanical analysis.

## Methods

### Animals

Male Wistar rats (weighing 250–300 g, $n=60$) were randomly assigned to one of two groups, control group (CG) or laser irradiated group (LG; $n=30$ each group). They were maintained under controlled temperature (24±2 °C), light–dark periods of 12 h, and with unrestricted access to water and commercial diet. All animal handling and surgical procedures were strictly conducted according the Guiding Principles for the Use of Laboratory Animals. This study was approved by the Animal Care Committee guidelines of the Federal University of São Carlos (002/2009). Rats were euthanized at 15, 30, and 45 days after surgery.

### Surgery

Bilateral noncritical size bone defects were surgically created on both tibias. The defect depth was guided until the rupture of cortical bone. The animals were anesthetized with ketamine/xilazine (80/10 mg/kg) and the midregions of the tibias were shaved and disinfected with povidone iodine. A dermoperiosteal incision was performed to expose the tibia. A standardized 3.0 mm diameter bone defect was created by using a motorized drill (BELTEC®, Araraquara, SP, Brazil; 13,500 rpm) under copious irrigation with saline solution. The cutaneous flap was replaced and sutured with resorbable polyglactin and the skin was disinfected with povidone iodine. The health status of the rats was monitored daily [1, 8, 9].

### Laser therapy

A low-energy Ga-Al-As laser, 830 nm (Teralaser, DMC®, São Carlos, SP, Brazil), continuous wavelength, 0.028 $cm^2$ spot area, 100 mW, 3.57 $W/cm^2$, 34 s, 3.4 J, and 120 $J/cm^2$ was used in this study. Laser irradiation started immediately after the surgery and it was repeated every 48 h, in a total of 8, 15, and 23 sessions, depending on the period of sacrifice (15, 30, and 45 days postsurgery, respectively). Laser irradiation was performed transcutaneously, at one point, above of the site of the injury (using the punctual contact technique). Animals were euthanized individually by carbon dioxide asphyxia. Both tibias were removed for analysis.

### Histopathological analysis

For the qualitative histopathological analysis, the right tibiae were used. They were removed, fixed in 10 % buffer formalin (Merck, Darmstadt, Germany), decalcified in 4 % EDTA (Merck), and embedded in paraffin blocks. Five-micrometer slices were obtained in a serially sectioned (longitudinally) pattern and stained with hematoxylin and eosin (H.E stain, Merck). Histopathological evaluation was performed (by a pathologist blinded to the treatment) under a light microscope (Olympus, Optical Co. Ltd, Tokyo, Japan; magnification of ×40). Any changes in the bone defect, such as presence of woven bone, bone marrow, inflammatory process, granulation tissue, or even tissues undergoing hyperplastic, metaplastic, and/or dysplastic transformation were investigated per animal.

### Morphometry analysis

All histological sections were quantitatively scored using computer-based image analysis techniques (Motican 5.0, Meiji camera, Santa Clara, CA, USA). The analysis was performed by two observers (CT and KNZ), in a blinded way. From digitalized images of the defect (×10), the amount of newly formed bone were determined within three regions of interest, i.e.: ROI1 (upper left border), ROI2 (lower left border), and ROI3 (central region of the right

border; Fig. 1). This analysis was established in a previous study conducted by our team [8, 9]. The amount of newly formed bone was determined in cubic micrometer in each ROI and the total newly formed bone was represented as ROI1+ROI2+ROI3.

## Immunohistochemistry

Paraffin was removed with xylene from serial sections of 4 μm and the sections were rehydrated in graded ethanol, then pretreated in a microwave with 0.01 M citric acid buffer (pH 6) for three cycles of 5 min each at 850 W for antigen retrieval. The material was preincubated with 0.3 % hydrogen peroxide in phosphate-buffered saline (PBS) solution for 5 min for inactivation of endogenous peroxidase and then blocked with 5 % normal goat serum in PBS solution for 10 min. The specimens were then incubated with anti-COX-2 polyclonal primary antibody (Santa Cruz Biotechnology, USA) at a concentration of 1:200, anti-RUNX-2 polyclonal primary antibody (Santa Cruz Biotechnology, USA) at a concentration of 1:200, anti-BMP-9 polyclonal primary antibody (Santa Cruz Biotechnology, USA) at a concentration of 1:200, and anti-RANKL polyclonal primary antibody (Santa Cruz Biotechnology, USA) at a concentration of 1:200. Incubation was carried out overnight at 4 °C within the refrigerator. This was followed by two washes in PBS for 10 min. The sections were then incubated with biotin conjugated secondary antibody antirabbit IgG (Vector Laboratories, Burlingame, CA, USA) at a concentration of 1:200 in PBS for 1 h. The sections were washed twice with PBS followed by the application of preformed avidin biotin complex conjugated to peroxidase (Vector Laboratories) for 45 min. The bound complexes were visualized by the application of a 0.05 % solution of 3-3′-diaminobenzidine solution and counterstained with Harris hematoxylin. For control studies of the antibodies, the serial sections were treated with rabbit IgG (Vector Laboratories) at a concentration of 1:200 in place of the primary antibody. Additionally, internal positive controls were performed with each staining bath.

COX-2, RUNX-2, BMP-9, and RANKL immunoexpressions were evaluated both qualitatively (presence of the immunomarkers) and quantitatively in five predetermined fields using a light microscopy (Leica Microsystems AG, Wetzlar, Germany) according to a previously described scoring scale from 1 to 4 (1=absent, 2=weak, 3=moderate, and 4=intense) for immunohistochemical analysis [10, 11]. The analysis was performed by two observers (CT and KNZ) in a blinded way.

## Biomechanical analysis

Biomechanical properties of the left tibia were determined by a three-point bending test with a 1 kN load (Instron® Universal Testing Machine, USA, 4444 model, 1 kN load cell). Tibiae were placed on a 3.8-cm metal device, which provided a 1.8 cm distance between the two supports. The load cell was perpendicularly positioned in the posterior–anterior direction at the exact site of the bone defect. A 5 N preload was applied in order to avoid specimen sliding. Finally, the bending force was applied at a constant deformation rate of 0.5 cm/min until fracture occurred. From the load deformation curve, the maximum load at failure (*N*) was obtained.

## Statistical analysis

The normality of all variables distribution was verified using Shapiro–Wilk's *W* test. For morphometry, immunohistochemical, and biomechanical analysis, comparisons among groups were performed using one-way analysis of variance, complemented by Duncan's post-test analysis. STATISTICA version 7.0 (data analysis software system—StatSoft Inc.) was

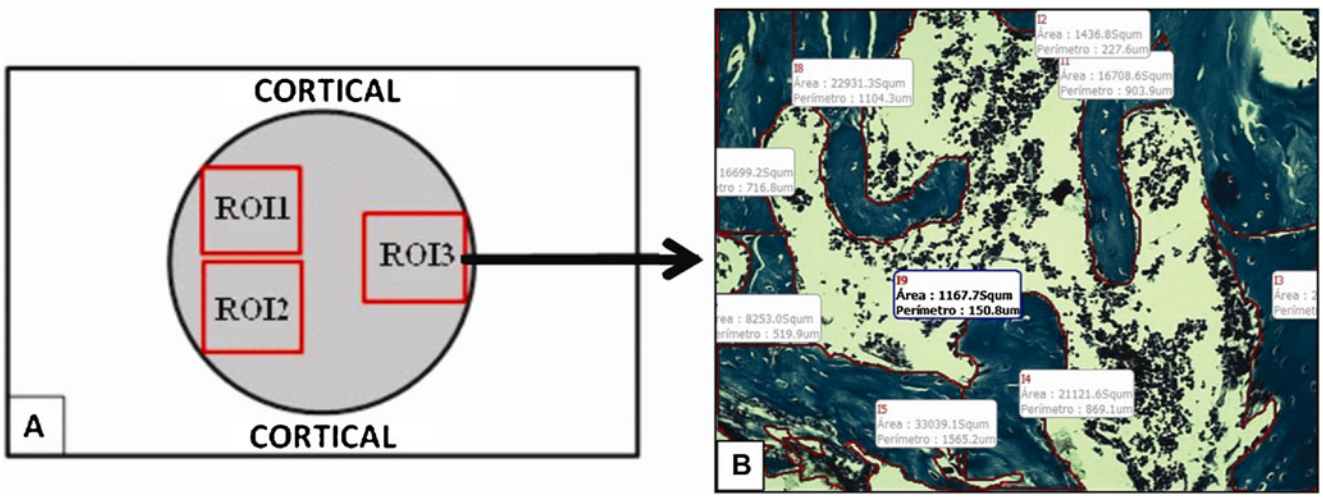


**Fig. 1** Morphometry of the area of new bone formation: **a** Illustration the standardization of fields selected for morphometric analysis. **b** Photomicrograph representative of the field 3 (*ROI3*) of defect in the control group 15 days. *Dark blue area* newly formed bone (masson trichrome)

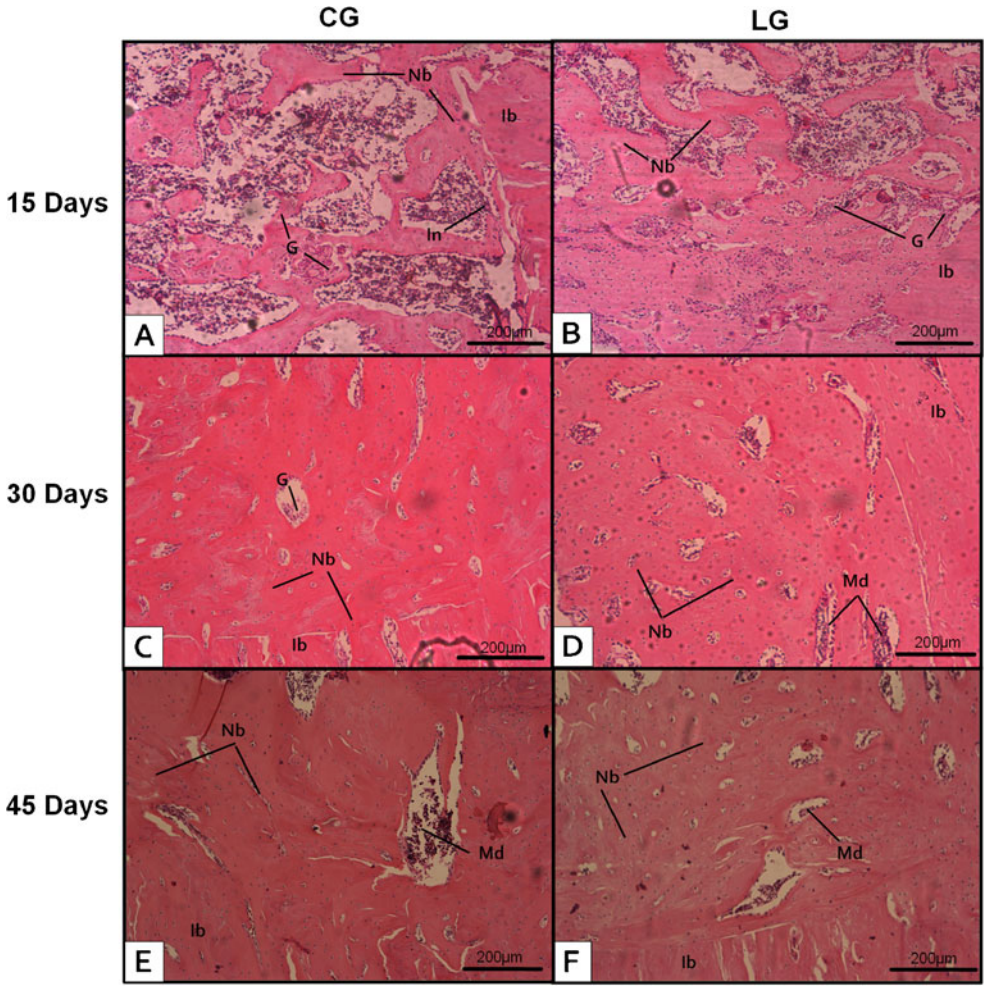


**Fig. 2** Representative histological sections of experimental groups. Intact bone (*Ib*), newly formed bone (*Nb*), medullar tissue (*Md*), granulation tissue (*G*), and inflammatory infiltrate (*In*). **a** Control group, 15 days; **b** laser irradiated group, 15 days; **c** control group, 30 days; **d** laser irradiated group, 30 days; **e** control group, 45 days; **f** laser irradiated group, 45 days (hematoxylin and eosin stain)

used to carry out the statistics analysis. Values of $p<0.05$ were considered statistically significant.

## Results

### General findings

Neither postoperative complications nor behavioral changes were observed. The rats returned rapidly to their normal diet and showed no loss of weight during the experimentation (data not shown). None of the animals died during the experiment and no infection in the surgical site was observed.

### Histological analysis

Figure 2 shows the histological findings of the control and laser irradiated groups, during the different experimental periods. Fifteen days postsurgery, the defects in the CG presented inflammatory infiltrate and minor amount of granulation tissue. Eventually, woven bone with no interconnected trabeculaes was observed. These histological results correspond to an initial phase of bone repair (Fig. 2a). The LG animals demonstrated mild delimitation of the borders of the injury, slight amount of granulation tissue, interconnected concentric trabeculaes, and no inflammatory infiltrate. Also, the animals of this group displayed a moderate amount of newly formed bone and a

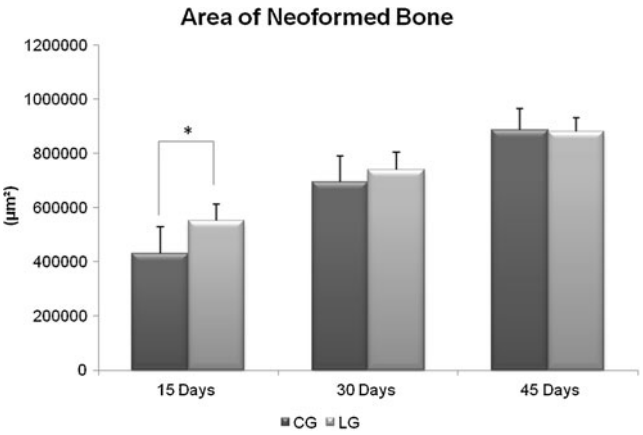


**Fig. 3** Means and SD of the newly formed bone tissue of bone area (square micrometer) of the defect after treatments. Significant differences of $p<0.05$ are represented by a single *asterisk*

better tissue organization compared to control, corresponding to a more advanced stage of bone repair (Fig. 2b).

On day 30 after surgery, the borders of the injury still could be observed in CG, with mild amount of newly formed bone and remodeling bone trabeculaes surrounded by granulation tissue (Fig. 2c). At the same period, laser irradiation produced moderate new bone formation, with the presence of high interconnected trabeculae and no granulation tissue, representing a more advanced stage of bone healing (Fig. 2d).

On day 45, no inflammatory process or granulation tissue were noticed in any specimens of CG and LG. In the CG, there was an intense presence of newly formed bone, with interconnected trabeculaes and organized tissue. In the animals of LG, we found similar characteristics as those described in the CG, corresponding to a final step of the bone healing (Fig. 2e and f).

## Morphometric analysis

Figure 3 shows the mean and standard deviation (SD) of the area of newly formed bone tissue during the experimental periods. Animals exposed to laser therapy presented a statistically higher area of newly formed bone compared to the CG at the first period evaluated ($p=0.0470$). However, no statistically significant differences between CG and LG were observed after 30 and 45 days postsurgery.

## Immunohistochemistry

In the first period analyzed, COX-2 expression was predominantly detected in the cytoplasm of bone cells. In the CG, immunoreactivity for COX-2 was mainly detected at the medullar tissue, whereas in the LG, a slight higher immunoexpression was evident in the cytoplasm of fibroblastic cells of granulation tissue and in cells of the medullar tissue (Fig. 4a and b). Thirty days after surgery, an immunoexpression of COX-2 was observed in osteocytes and osteoblasts for both CG and LG (Fig. 4c and d). At the 45th day postsurgery, no immunoexpression of COX-2 was observed for CG and LG (Fig. 4e and f).

The labeling for RUNX-2 was initially observed mainly at the medullar tissue for both CG and LG (Fig. 5a and b). Thirty days after surgery, both CG and LG showed an immunoexpression of RUNX-2 in the cytoplasm of

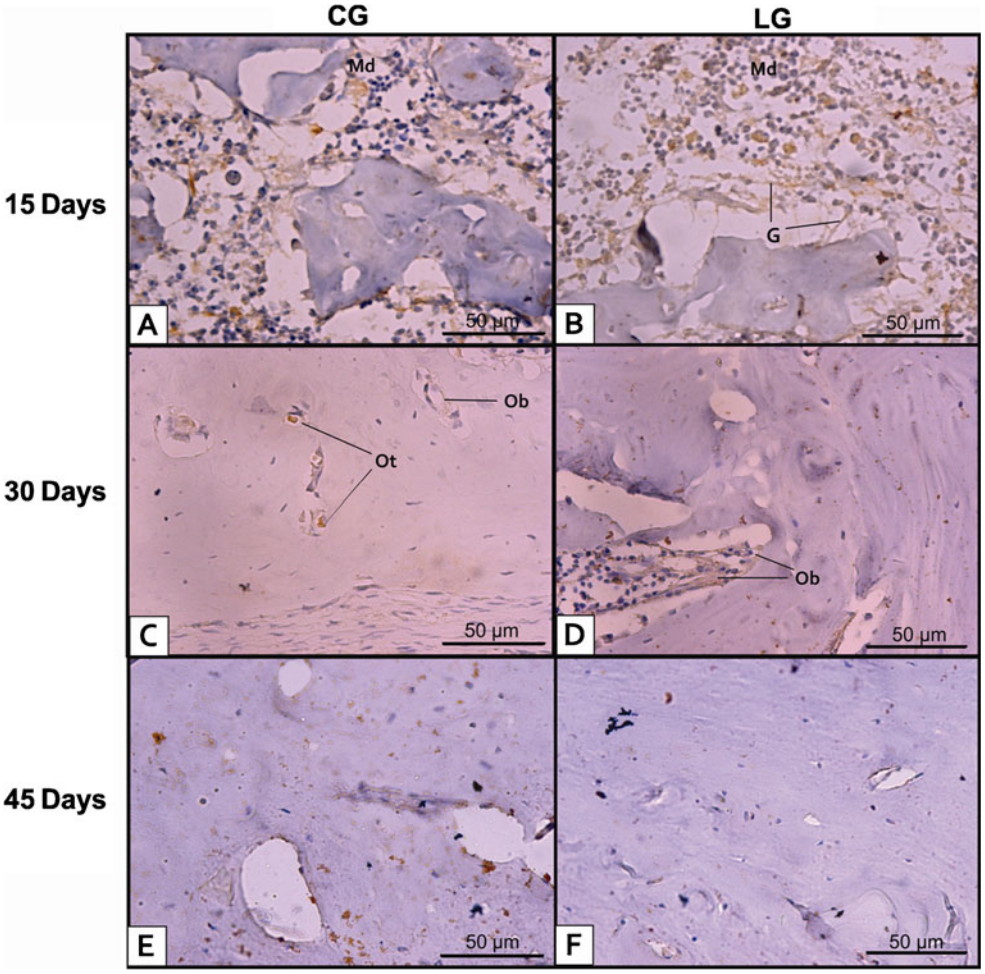


**Fig. 4** Representative sections of COX-2 immunohistochemistry. Medullar tissue (*Md*), cytoplasm of fibroblastic cells of granulation tissue (*G*), osteocytes (*Ot*), and osteoblasts (*Ob*). **a** Control group, 15 days; **b** laser irradiated group, 15 days; **c** control group, 30 days; **d** laser irradiated group, 30 days; **e** control group, 45 days; **f** laser irradiated group, 45 days

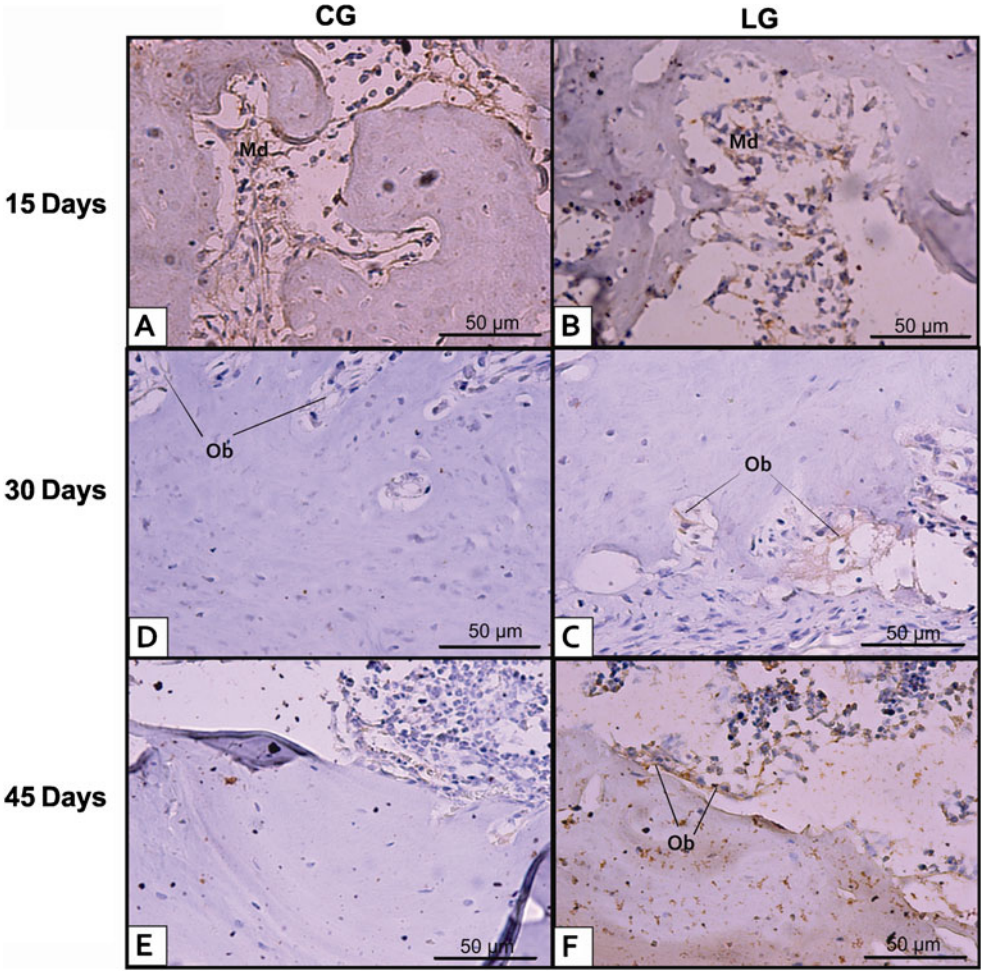


**Fig. 5** Representative sections of RUNX-2 immunohistochemistry. Medullar tissue (*Md*), cytoplasm of osteoblasts (*Ob*). **a** Control group, 15 days; **b** laser irradiated group, 15 days; **c** control group, 30 days; **d** laser irradiated group, 30 days; **e** control group, 45 days; **f** laser irradiated group, 45 days

osteoblasts (Fig. 5c and d). At the last period evaluated in the study, no immunoexpression of RUNX-2 was observed in the CG (Fig. 5e). However, a slight immunolabeling of RUNX-2 was still observed in osteoblasts of the LG (Fig. 5f).

Fifteen days after surgery, the immunoexpression of BMP-9 could be observed mainly at the medullar tissue in the CG and LG (Fig. 6a and b). At 30 days postsurgery, the BMP-9 immunoexpression was found in the cytoplasm of osteoblasts in the CG and LG (Fig. 6c and d). However, there was no expressivity for this immunomarker both in the CG and LG at the day 45 postsurgery (Fig. 6e and f).

The labeling for RANKL was predominantly observed at the medullar tissue in both groups at 15 days postsurgery (Fig. 7a and b). Thirty and 45 days after surgery, the immunoexpression of RANKL was mainly identified in granulation tissue in CG and osteoblastic cells in LG (Fig. 7c and d).

### Quantitative analysis

Similar findings for COX-2 immunoexpression were observed in CG and LG at the different experimental periods analyzed (Fig. 8a). The labeling for RUNX-2 occurred in the CG and LG groups equally, without any significant differences among groups at days 15 and 30 postsurgery. At the last set point evaluated in this study, the expression of RUNX-2 was significantly higher in LG than in CG ($p$=0.0001; Fig. 8b). Fifteen days postsurgery, similar response to BMP-9 was noted for both groups, but a significantly higher BMP-9 expression was observed in LG when compared to CG 30 days postsurgery ($p$=0.0171) and no difference was found in the last experimental period (Fig. 8c). No statistically significant differences were detected among the groups when considering the same period for RANKL expression (Fig. 8d).

### Biomechanical analysis

Figure 9 shows the means and SD of the biomechanical test of all groups. No statistically significant difference among the groups was observed for the variable maximal load in any period of time.

## Discussion

The present study investigated the effects of LLLT on the histology, morphometry, immunoexpression of osteogenic

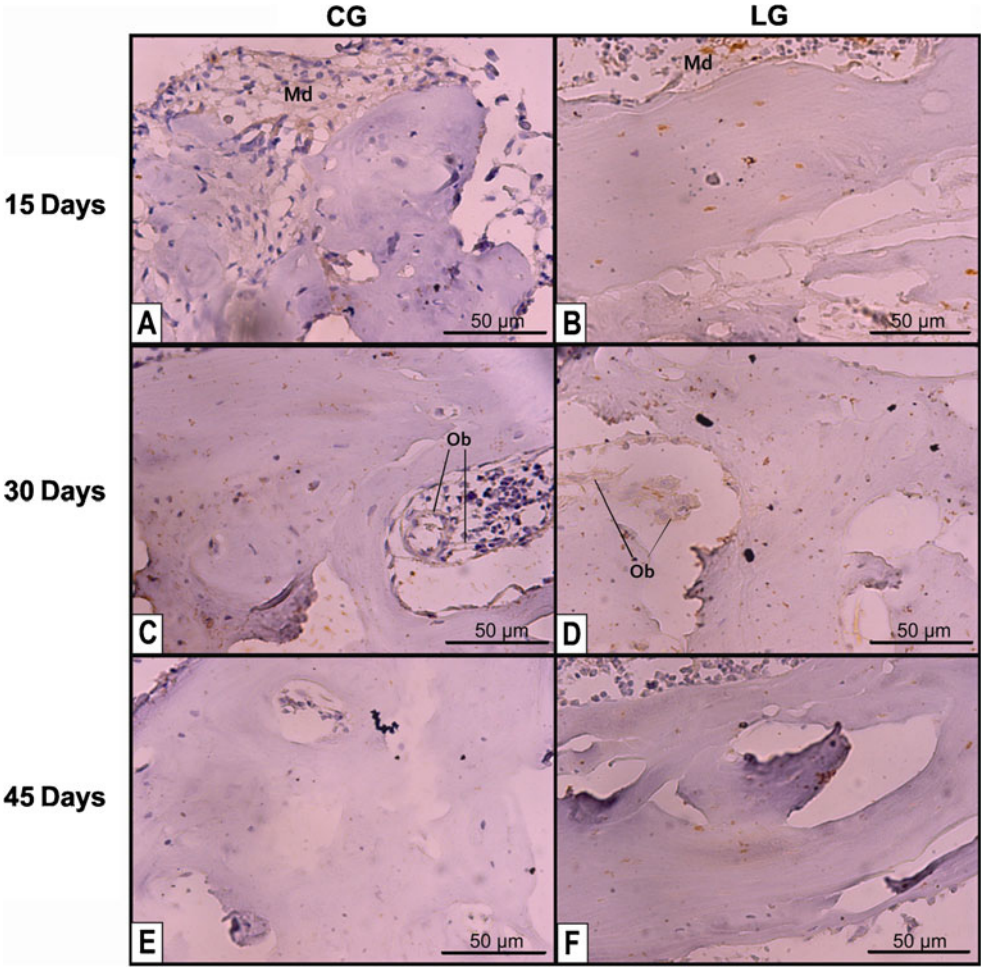


**Fig. 6** Representative sections of BMP-9 immunohistochemistry. Medullar tissue (*Md*), cytoplasm of osteoblasts (*Ob*). **a** Control group, 15 days; **b** laser irradiated group, 15 days; **c** control group, 30 days; **d** laser irradiated group, 30 days; **e** control group, 45 days; **f** laser irradiated group, 45 days

factors (COX-2, RUNX-2, BMP-9, and RANKL), and biomechanical properties of the tibial callus during the process of bone healing in a tibial bone defect model in rats. To the best of our knowledge, this approach has not been demonstrated so far.

The histological analysis revealed that laser therapy improved the biological response of bone tissue by stimulating the deposition of newly formed bone at the site of the injury. It seems that laser irradiation is able to modulate cell biochemical reactions and stimulate mitochondrial respiration, with the consumption of molecular oxygen and ATP synthesis [12, 13]. These effects can increase the synthesis of DNA, RNA, and cell cycle regulatory proteins, thus promoting cell proliferation [14]. In bone, LLLT has a stimulatory effect and can increase cell proliferation and accelerate fracture consolidation [4]. The positive histological findings observed in this study in the treated groups are probably related to the stimulation of osteogenic genes and protein expression by laser irradiation through the mechanisms aforementioned. The upregulation of these factors could be related with the attraction of the osteoprogenitor cells and their differentiation into matrix-producing osteoblasts, thus increasing the rate of bone formation and bone ingrowth into the defect area [3].

Also, in this study, a peak of expression of COX-2 was observed in LG and CG at day 15 after surgery, followed by a temporal decrease. The expression of COX-2 is relevant to many processes. Specifically in bone healing, elevated COX-2 expression increases the differentiation of mesenchymal stem cells into osteoblasts in response to osteogenic signals [7]. It is possible that the increased appearance of COX-2 in the irradiated animals (followed by the decrease of the expression of this marker) could have contributed to the earlier recruitment of pre-osteoblasts and osteoblasts, thus culminating in the presence of a more organized tissue and an earlier deposition of newly formed bone.

In addition, RUNX-2 immunoexpression analysis revealed the presence of this immunomarker in the LG at all experimental periods, with a statistically higher immunolabeling in comparison to CG at the last period evaluated. It is known that RUNX-2 is predominantly expressed in osteoblasts and is obligatory for commitment of mesenchymal progenitors to the osteoblast lineage. Moreover, RUNX-2 is essential for the upregulation of other osteoblastic markers such as osteocalcin, osteopontin, alkaline phosphatase, and collagen type I [15]. Taken as a whole, it seems that the expression of RUNX-2 in all periods evaluated, with a peak of expression at

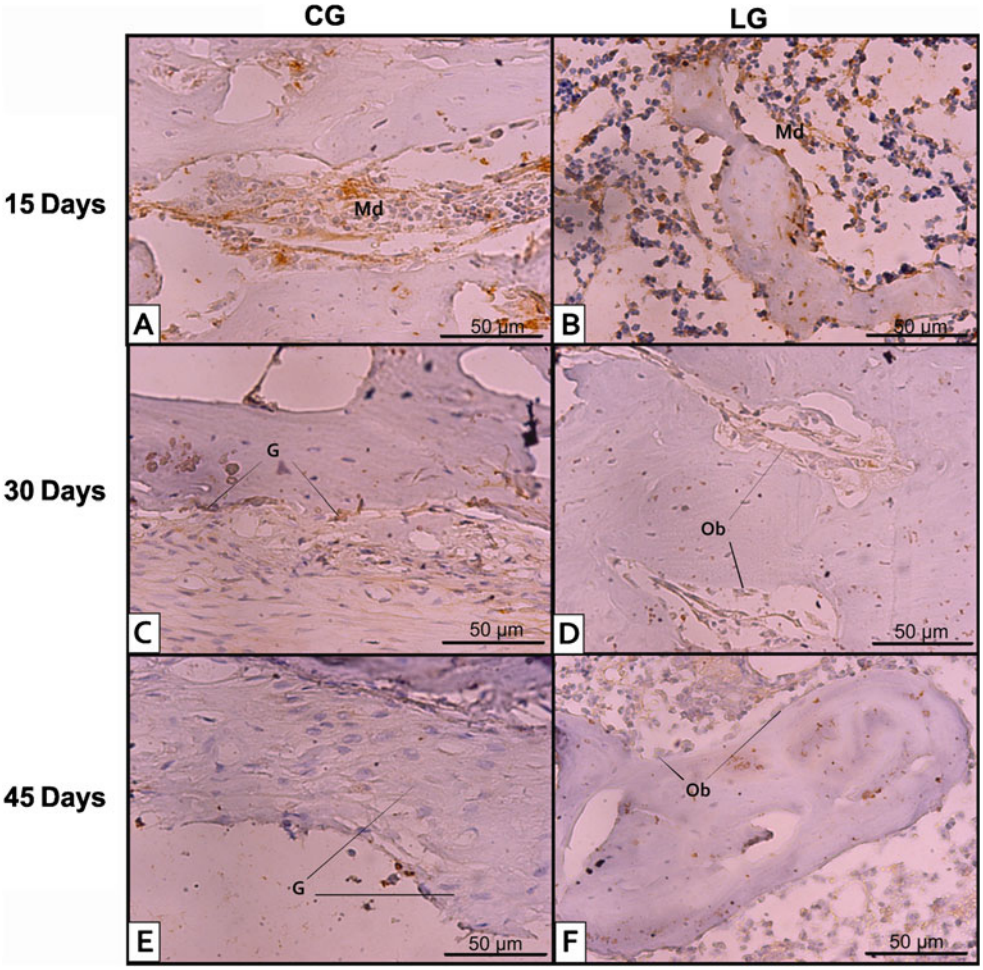


**Fig. 7** Representative sections of RANKL immunohistochemistry. Medullar tissue (*Md*), cytoplasm of fibroblastic cells of granulation tissue (*G*), osteoblasts (*Ob*). **a** Control group, 15 days; **b** laser irradiated group, 15 days; **c** control group, 30 days; **d** laser irradiated group, 30 days; **e** control group, 45 days; **f** laser irradiated group, 45 days

day 45, could be related to the more organized newly formed bone observed in the laser irradiated animals, thus supporting the hypothesis that laser therapy shows an osteogenic potential.

BMPs are other essentials factors related to the osteoblast differentiation and bone regeneration [16]. In addition, it has recently been shown that BMP-9 is one of the most potent osteoindutive BMPs [17]. In this study, laser therapy produced a statistically higher BMP-9 expression in LG compared to CG 30 days postsurgery. Probably, the upregulation of BMP-9 in the treated group was responsible for the earlier recruitment of cells observed in the histological analysis in this group, which may be a result of a higher number of mature osteoblasts and a higher deposition of neoformed bone. These in vivo findings are in agreement with previous in vitro studies which have shown that LLLT (Ga-Al-As, 830 nm, 1.91 J/cm$^2$) stimulated in vitro mineralization via increased gene and protein expression of BMPs 2, 4, 6, and 7 and RUNX-2 in MC3T3-E1 mouse osteoblast-like cells [5].

Also, an appropriate bone healing process includes bone remodeling, which involves the resorption of bone by osteoclasts and synthesis of bone matrix by osteoblasts [18, 19]. In this context, the action of osteoclasts and the factors that stimulate their differentiation and function are crucial for the healing process. Recently, RANKL has been identified as a very important osteoclast differentiation and activation factor [20]. In this study, the control group and laser irradiated group showed a positive immunoexpression of RANKL during all set points evaluated. An in vitro study showed that LLLT (Ga-Al-As, 810 nm, 27.99 J/cm$^2$) stimulated RANK expression in osteoclast precursor cells at an early stage when compared to the control group [21].

Despite the marked stimulatory effects of LLLT on the histological and immunohistochemical analysis during the process of bone healing, no statistically significant difference in the biomechanical analysis was found comparing the treated and control groups. Bone mass, as well as the quality and arrangement of its microstructural elements, influences bone mechanical properties [8]. Therefore, the lack of the improved load-bearing capacity showed by the laser-treated group probably mirrors the lack of difference in the spatial distribution of newly formed bone into the defect site among the groups. These results are in agreement with those observed by Shakouri et al.[22], who showed that the 780 nm laser (Ga-Al-As, 4 J/cm$^2$) enhanced callus development in the early stage of the healing process (2 and 5 weeks postoperative),

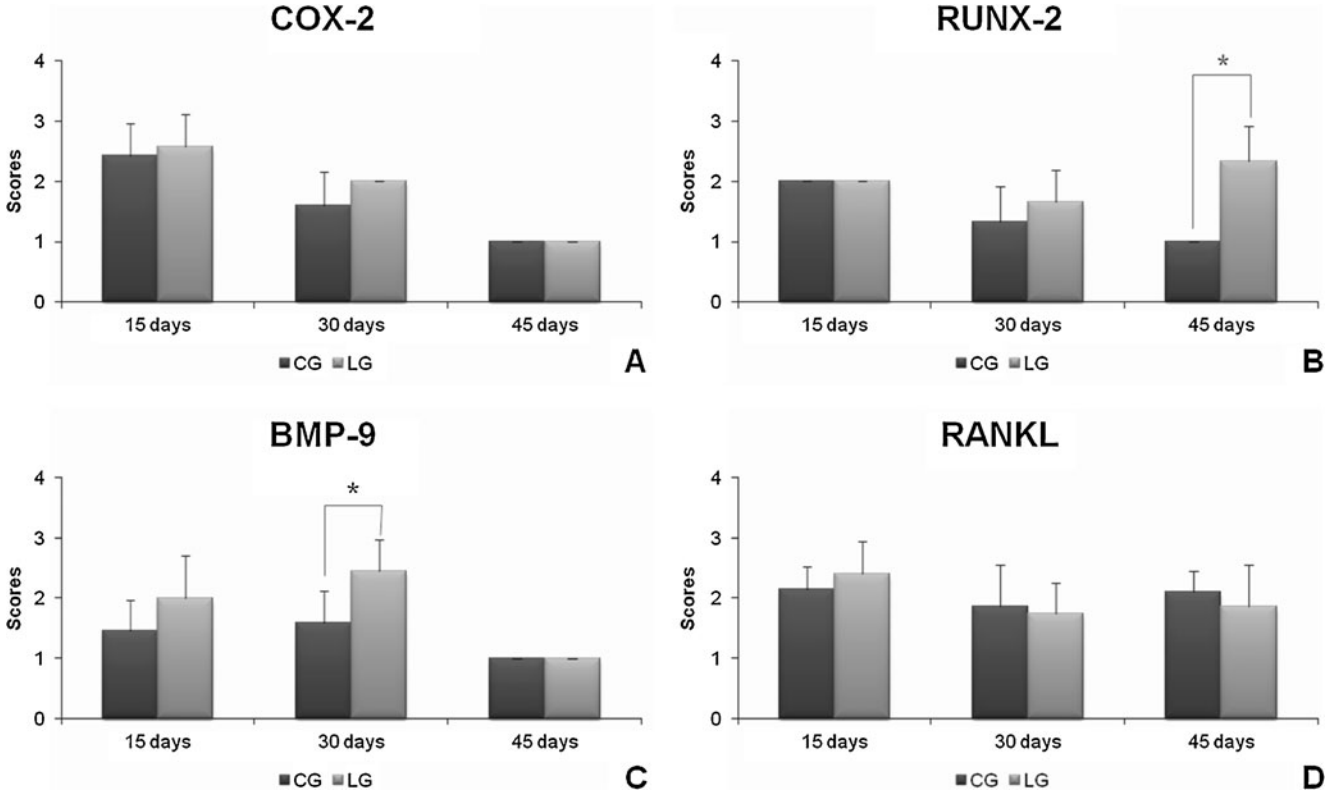


**Fig. 8** Means and SD scores of immunohistochemistry. **a** COX-2, **b** RUNX-2, **c** BMP-9, **d** RANKL. *CG* control group, *LG* laser irradiated group. Significant differences of $p<0.05$ are represented by a single *asterisk*

but with no improvement in the biomechanical properties of the healing bone. At the same way, Oliveira et al. [9] found no statistically difference in the maximum load and energy absorption in the callus of rats treated with 830 nm laser and the control group. Conversely, Luger et al. [23] (He-Ne, 632.8 nm, 35 mW) and Lirani-Galvão et al. [1] (Ga-Al-As, 780 nm, 112.5 J/cm$^2$) observed an increase in the biomechanical properties of tibial callus in rats after laser irradiation. However, it is noteworthy that these studies used different experimental models, dosimetric parameters, and wavelengths compared to those used in the present work.

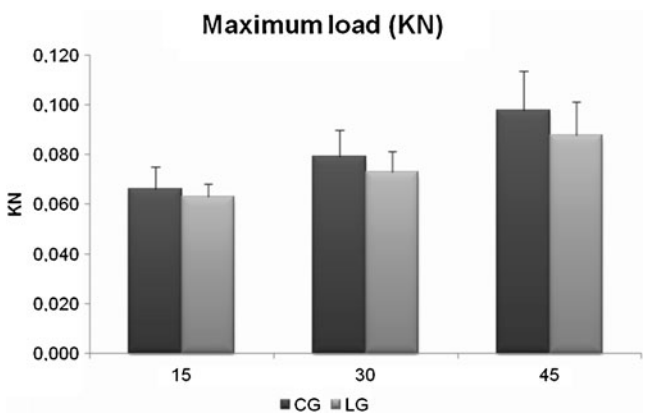


**Fig. 9** Means and SD of maximum load

Our results corroborate those of Shakouri et al.[22], who showed that the 780 nm laser (Ga-Al-As, 4 J/cm$^2$) enhanced callus development in the early stage of the healing process (2 and 5 weeks postoperative), but with no improvement in the biomechanical properties of the healing bone. At the same way, Oliveira et al. [9] found no statistically difference in the maximum load and energy absorption in the callus of rats treated with 830 nm laser and the control group. Conversely, Luger et al. [23] (He-Ne, 632.8 nm, 35 mW) and Lirani-Galvão et al. [1] (Ga-Al-As, 780 nm, 112.5 J/cm$^2$) observed an increase in the biomechanical properties of tibial callus in rats after laser irradiation. However, it is noteworthy that these studies used different experimental models, dosimetric parameters, and wavelengths compared to those used in the present work.

Some limitations of this work should be pointed out. We investigated the effects of LLLT on bone healing at 15, 30, and 45 days postsurgery. It would be interesting to investigate the early response to the laser application about expression of osteogenic factors COX-2, RUNX-2, BMP-9, and RANKL. Also, more quantitative analysis should be included in future research such as the quantification of inflammatory cells on immunohistochemical analysis.

In spite of these limitations, the results of this work highlight the stimulatory effects of laser therapy on bone healing. Such findings would allow us to obtain relevant data on the

potential of this therapy to be used as an effective treatment for non-union fractures or pseudoarthrosis. However, the reasons for the stimulatory effects of LLLT and the better parameters to be used in clinical therapies warrant further investigation.

## Conclusion

In summary, our findings indicate that the laser therapy improved bone healing process by accelerating the deposition and organization of newly formed bone and activating osteogenic factors as RUNX-2 and BMP-9 on created bone defects in tibias of rats.

**Acknowledgments** We thank the Brazilian funding agencies Fapesp and CNPq for the financial support of this research.

## References

1. Lirani-Galvão AP, Jorgetti V, da Silva OL (2006) Comparative study of how low-level laser therapy and low-intensity pulsed ultrasound affect bone repair in rats. Photomed Laser Surg 24:735–740
2. Rennó ACM, Mcdonnell PA, Parizotto NA, Laakso EL (2007) The effects of laser irradiation on osteoblast and osteosarcoma cell proliferation and differentiation in vitro. Photomed Laser Surg 25:275–280
3. Fávaro-Pipi E, Ribeiro DA, Ribeiro JU, Bossini P, Oliveira P, Parizotto NA, Tim C, Araújo HSS, Rennó ACM (2011) Low-level laser therapy induces differential expression of osteogenic genes during bone repair in rats. Photomed Laser Surg 9:311–317
4. Fávaro-Pipi E, Feitosa SM, Ribeiro DA, Bossini P, Oliveira P, Parizotto NA, Rennó ACM (2010) Comparative study of the effects of low-intensity pulsed ultrasound and low-level laser therapy on bone defects in tibias of rats. Lasers Med Sci 25:727–732
5. Fujimoto K, Kiyosaki T, Mitsui N, Mayahara K, Omasa S, Suzuki N, Shimizu N (2010) Low-intensity laser irradiation stimulates mineralization via increased BMPs in MC3T3-E1 cells. Lasers Surg Med 42:519–526
6. Kiyosaki T, Mitsui N, Suzuki N, Shimizu N (2010) Low-level laser therapy stimulates mineralization via increased RUNX-2 expression and ERK phosphorylation in osteoblasts. Photomed Laser Surg 28:S16–S172
7. Ribeiro DA, Matsumoto MA (2008) Low-level laser therapy improves bone repair in rats treated with anti-inflammatory drugs. J Oral Rehabil 35:925–933
8. Oliveira P, Ribeiro DA, Pipi EF, Driusso P, Parizotto NA, Rennó AC (2010) Low-level laser therapy does not modulate the outcomes of a highly bioactive glass-ceramic (Biosilicate) on bone consolidation in rats. J Mater Sci Mater Med 21:1379–1384
9. Bossini PS, Rennó ACM, Ribeiro DA, Fangel R, Peitl O, Zanotto ED, Parizotto NA (2011) Biosilicate® and low-level laser therapy improve bone repair in osteoporotic rats. J Tissue Eng Regen Med 5:229–237
10. Pedrosa WF Jr, Okamoto R, Faria PE, Arnez MF, Xavier SP, Salata LA (2009) Immunohistochemical, tomographic and histological study on onlay bone graft remodeling. Part II: calvarial bone. Clin Oral Implants Res 20:1254–64
11. Mariza Akemi Matsumoto MA, Holgado LA, Renno ACM, Caviquioli G, Biguetti CC, Saraiva PP, Kawakami RY (2012) A novel bioactive vitroceramic presents similar biological responses as autogenous bone grafts. J Mater Sci Mater Med 23:1447–1456
12. Pires Oliveira DA, de Oliveira RF, Zangaro RA, Soares CP (2008) Evaluation of low-level laser therapy of osteoblastic cells. Photomed Laser Surg 26:401–404
13. Garavello-Freitas I, Baranauskas V, Joazeiro P, Padovani CR, Pai-Silva MD, Cruz-Hofling MA (2003) Low-power laser irradiation improves histomorphometrical parameters and bone matrix organization during tibia wound healing in rats. J Photochem Photobiol 70:81–9
14. Stein A, Benayahu D, Maltz L, Oron U (2005) Low level laser irradiation promotes proliferation and differentiation of human osteoblasts in vitro. Photomed Laser Surg 23:161–166
15. Zhang X, Schwarz EM, Young DA, Puzas E, Rosier RN, O'keefe RJ (2002) Cyclo-oxygenase-2 regulates mesenchymal cell differentiation into the osteoblast lineage and is critically involved in bone repair. J Clin Invest 109:1405–1415
16. Proff P, Römer P (2009) The molecular mechanism behind bone remodelling: a review. Clin Oral Investig 13:355–362
17. Kang Q, Sun MH, Cheng H, Peng Y, Montag AG, Deyrup AT, Jiang W, Luu HH, Luo J, Szatkowski VP, Park JY, Li Y, Haydon RC, He TC (2004) Characterization of the distinct orthotopic bone-forming activity of 14 BMPs using recombinant adenovirus-mediated gene delivery. Gene Ther 11:1312–1320
18. Rodan GA (1996) Coupling of bone resorption and formation during bone remodeling. In: Marcus R, Feldman D, Kelsey J (eds) Osteoporosis. Academic Press, San Diego, CA, pp 289–299
19. Lemaire V, Tobin FL, Greller LD, Cho CR, Suva LJ (2004) Modeling the interactions between osteoblast and osteoclast activities in bone remodeling. J Theor Biol 229:293–309
20. Anderson DM, Maraskovsky E, Billingsley WL, Dougall WC, Tometsko ME, Roux ER, Teepe MC, Dubose RF, Cosman D, Galibert L (1997) A homologue of the TNF receptor and its ligand enhance T-cell growth and dendritic-cell function. Nature 390:175–179
21. Aihara N, Yamaguchi M, Kasai K (2006) Low-energy irradiation stimulates formation of osteoclast-like cells via RANK expression in vitro. Lasers Med Sci 21:24–33
22. Shakouri SK, Soleimanpour J, Salekzamani Y, Oskuie MR (2009) Effect of low-level laser therapy on the fracture healing process. Lasers Med Sci 15:240–244
23. Luger EJ, Rochkind S, Wollman Y, Kogan G, Dekel S (1998) Effect of low-power laser irradiation on the mechanical properties of bone fracture healing in rats. Lasers Surg Med 22:97–102